Inorg. Chem. **2005**, *44*, 2272–2281

Structure and Physical Properties of Ternary Rare-Earth Cobalt Bismuth Intermetallics $(RE)_{12}Co_5Bi$ (RE = Y, Gd, Tb, Dy, Ho, Er, Tm)

Andriy V. Tkachuk and Arthur Mar*

Department of Chemistry, University of Alberta, Edmonton, Alberta, Canada T6G 2G2

Received December 21, 2004

The rare-earth intermetallic compounds $(RE)_{12}Co_5Bi$ (RE = Y, Gd, Tb, Dy, Ho, Er, Tm) were prepared by arc-melting and annealing at 600 °C. These compounds extend the previously known $(RE)_6M_{2+x}X_{1-x}$ (M = Co, Ni; X = Ga, In, Sn, Pb) series with the Ho_6Co_2Ga-type structure to X = Bi. The crystal structure of $Ho_{12}Co_5Bi$ was refined by the Rietveld method from powder X-ray diffraction data obtained using synchrotron radiation (Pearson symbol *oI*36, orthorhombic, space group *Immm*, $Z = 2$, $a = 9.37598(14)$ Å, $b = 9.37871(14)$ Å, $c = 9.85465(13)$ Å). Unlike other Ho_6Co_2Ga-type compounds, the 2a site in $Ho_{12}Co_5Bi$ is exclusively occupied by Co atoms. Four-probe electrical resistivity measurements on sintered polycrystalline samples of $(RE)_{12}Co_5Bi$ indicated metallic behavior. Magnetic measurements revealed behavior ranging from frequency-dependent maxima in the ac susceptibility for $Y_{12}Co_5Bi$ to possible ferrimagnetic ordering for $Gd_{12}Co_5Bi$ to antiferromagnetic ordering with metamagnetic transitions for the remaining compounds. As confirmed by band structure calculations using $Y_{12}Co_5Bi$ as a model compound, Y–Y and Y–Co interactions are the most important bonding components, but matrix effects are likely responsible for anomalously short Co–Co contacts in the structure.

Introduction

A class of rare-earth intermetallic compounds having the composition $(RE)_6M_{2+x}X_{1-x}$ (RE = later rare earths; M = Co, Ni; X = Ga, In, Sn, Pb) has been identified previously.[1−9] Given the potential for complex electrical and magnetic behavior arising from the coupling of f and d electrons in rare-earth transition-metal intermetallic compounds, the properties for some of these compounds, especially the stannides, have begun to be investigated. For example, magnetic data for Er_6Ni_2Sn or $Tb_6Co_{2.35}Sn_{0.65}$ reveal anomalies suggestive of the presence of several magnetic phases.[7−9] The parent structure type is known as the Ho_6Co_2Ga type, in which the rare-earth atoms form a metal−metal-bonded framework defining several types of high-coordination polyhedra that encapsulate the transition-metal and p-block atoms.[1] Depending on the relative sizes of the M and X atoms, there is a possibility for disorder within these sites. We wondered whether exaggerating these size differences would prevent disorder from occurring and induce preferential occupation of these sites. Because of our ongoing interest in ternary rare-earth compounds of the heavier pnicogens, we chose to target the preparation of $(RE)_6Co_{2+x}Bi_{1-x}$ and $(RE)_6Ni_{2+x}Bi_{1-x}$, with the expectation that the much larger Bi atom would prefer to occupy certain sites. Although the ternary RE−M−Sb (RE = rare earth; M = transition metal) systems have provided much fodder for new materials,[10] comparatively less is known about the corresponding RE−M−Bi systems. For example, in the RE−Co−Bi systems, $(RE)_6Co_{13}Bi$ ($La_6Co_{11}Ga_3$-type) and $(RE)_6CoBi_2$ (Zr_6CoAs_2-type) phases are known.[11,12] Although it has a

* Author to whom correspondence should be addressed. E-mail: arthur.mar@ualberta.ca.

(1) Gladyshevskii, R. E.; Grin', Yu, M.; Yarmolyuk, Ya. P. *Dopov. Akad. Nauk Ukr. RSR, Ser. A: Fiz.-Mat. Tekh. Nauki* **1983**, *2*, 67−70.
(2) Sichevich, O. M.; Komarovskaya, L. P.; Grin', Yu. N.; Yarmolyuk, Ya. P.; Skolozdra, R. V. *Ukr. Fiz. Zh. (Russ. Ed.)* **1984**, *29*, 1342−1345.
(3) Kalychak, J. M.; Zaremba, V. I.; Zavalij, P. Y. *Z. Kristallogr.* **1993**, *208*, 380−381.
(4) Kalychak, Ya. M. *J. Alloys Compd.* **1999**, *291*, 80−88.
(5) Gulay, L. D.; Wołcyrz, M. *J. Alloys Compd.* **2001**, *315*, 164−168.
(6) Dremov, R. V.; Koblyuk, N.; Mudryk, Ya.; Romaka, L.; Sechovský, V. *J. Alloys Compd.* **2001**, *317−318*, 293−296.
(7) Syshchenko, O.; Stadnyk, Yu.; Romaka, L.; Mudryk, Ya.; Dremov, R. V.; Sechovský, V. *J. Alloys Compd.* **2001**, *319*, 14−18.
(8) Kolomiets, A. V.; Mudryk, Ya.; Stadnyk, Yu.; Sechovský, V. *J. Alloys Compd.* **2002**, *333*, 34−40.
(9) Babyuk, V.; Staszczuk, P.; Bodak, O.; Gorelenko, Yu.; Romaka, L.; Stadnyk, Yu. *J. Alloys Compd.* **2004**, *365*, 21−24.
(10) Sologub, O. L.; Salamakha, P. S. In *Handbook on the Physics and Chemistry of Rare Earths*; Gschneidner, K. A., Jr., Bünzli, J.-C. G., Pecharsky, V. K., Eds.; Elsevier: Amsterdam, 2003; pp 35−146.
(11) Weitzer, F.; Leithe-Jasper, A.; Rogl, P.; Hiebl, K.; Noël, H.; Wiesinger, G.; Steiner, W. *J. Solid State Chem.* **1993**, *104*, 368−376.
(12) Morozkin, A. V. *J. Alloys Compd.* **2003**, *360*, L7−L8.

10.1021/ic048195p CCC: $30.25
Published on Web 02/24/2005

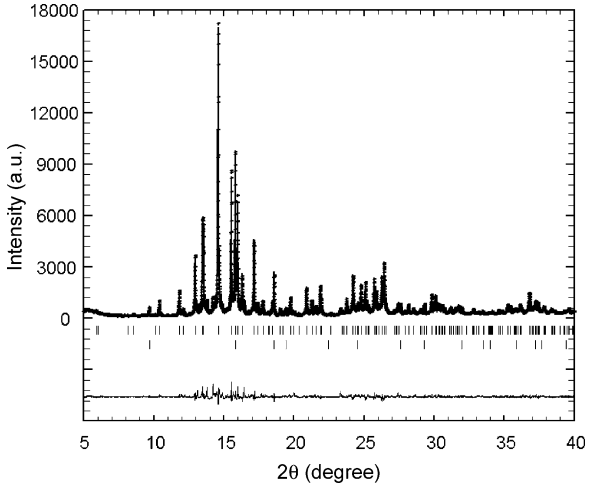

Figure 1. Rietveld refinement results for $Ho_{12}Co_5Bi$. The observed profile is indicated by plus signs and the calculated profile by the solid line. The top set of vertical tic marks corresponds to the Bragg peak positions for $Ho_{12}Co_5Bi$ and the bottom set to those of trace amounts of $HoCo_2$. The difference plot is shown at the bottom.

similar composition, the latter structure type is unrelated to the Ho_6Co_2Ga type, being based instead on an Fe_2P-type superstructure, in which filled trigonal prisms form the characteristic motif.

The synthesis of seven new compounds $(RE)_{12}Co_5Bi$ (or $(RE)_6Co_{2.5}Bi_{0.5}$) (RE = Y, Gd, Tb, Dy, Ho, Er, Tm) is presented here. The crystal structure of $Ho_{12}Co_5Bi$ has been determined and is compared with those of other rare-earth-rich intermetallic compounds such as Ho_6Co_2Ga and $Ho_6Co_{2+x}In_{1-x}$. The electrical and magnetic properties of these compounds are described. The bonding in the model compound $Y_{12}Co_5Bi$ is analyzed through band structure calculations.

Experimental Section

Synthesis. Starting materials were powders of the rare-earth elements (99.9%, Alfa-Aesar), cobalt (99.8%, Cerac), and bismuth (99.999%, Alfa-Aesar). Cold-pressed pellets (~0.25 g) were prepared from the stoichiometric amounts of elemental components. The original intent was to prepare compounds with a hypothetical "$(RE)_{12}Co_6Bi$" stoichiometry, analogous to $Sm_{12}Ni_6In$-type compounds.[9,13−15] In an Edmund Bühler MAM-1 compact arc melter on a water-cooled copper bottom under an argon atmosphere, pellets of this composition were arc-melted and then annealed in sealed evacuated silica tubes at 870 K for 720 h. Analysis of the powder X-ray diffraction pattern for the product of an arc-melting reaction, "$Ho_{12}Co_6Bi$", revealed that the major phase formed was instead the new phase $Ho_{12}Co_5Bi$, with traces of $HoCo_2$ (Figure 1). After the structure and composition were determined unequivocally, efforts were subsequently made to optimize the synthesis of phase-pure samples of $(RE)_{12}Co_5Bi$. It is important to add an excess of 5 wt % bismuth to compensate for evaporative loss during arc-melting of reactions with the composition "$(RE)_{12}Co_5Bi$". After the resulting ingots were annealed in sealed evacuated silica tubes at 870 K for 720 h and then quenched in cold water, phase-pure polycrystalline samples of $(RE)_{12}Co_5Bi$ (RE = Y, Gd, Tb, Dy, Ho, Er, Tm) were obtained.

Table 1. Cell Parameters for $(RE)_{12}Co_5Bi$[a]

compound	a (Å)	b (Å)	c (Å)	V (Å^3)
$Y_{12}Co_5Bi$	9.524(3)	9.533(3)	9.952(2)	903.6(3)
$Gd_{12}Co_5Bi$	9.602(4)	9.623(4)	10.054(3)	929.0(4)
$Tb_{12}Co_5Bi$	9.502(3)	9.519(3)	9.989(2)	903.5(3)
$Dy_{12}Co_5Bi$	9.459(3)	9.471(3)	9.949(2)	891.3(3)
$Ho_{12}Co_5Bi$	9.387(1)	9.393(1)	9.884(1)	871.5(1)
$Er_{12}Co_5Bi$	9.327(1)	9.328(1)	9.836(1)	855.6(1)
$Tm_{12}Co_5Bi$	9.272(2)	9.276(2)	9.791(2)	842.0(2)

[a] Refined from Guinier data.

The arc-melted ingots of the ternary compounds have metallic luster; the powders are gray and are stable in air. Energy-dispersive X-ray (EDX) analyses on a Hitachi S-2700 scanning electron microscope were in good agreement with the ideal composition and did not show the presence of any impurity elements. All samples were characterized by powder X-ray diffraction on an Enraf-Nonius FR552 Guinier camera, recorded with Cu $K\alpha_1$ radiation (λ = 1.54056 Å) using silicon as an external standard. Cell parameters for ternary $(RE)_{12}Co_5Bi$ (RE = Y, Gd, Tb, Dy, Ho, Er, Tm) compounds are listed in Table 1. Attempts were made to prepare the corresponding Ni compounds $(RE)_{12}Ni_5Bi$ but to no avail.

Structure Determination. Intensity data for $Ho_{12}Co_5Bi$ were collected on the SUNY X3 beamline at the National Synchrotron Light Source at Brookhaven National Laboratory with 0.6995 Å radiation. Structure refinements were carried out with the full-profile Rietveld method using the program FULLPROF.[16] Further details of the data collection and structure refinement are summarized in Table 2. (The superior resolution of the synchrotron data leads to smaller uncertainties in the cell parameters; however, the deviation from the values refined from Guinier data shown in Table 1 may reflect slight differences in the sample composition, perhaps from a small range of homogeneity.) Initial atomic positions were taken from the structure of Ho_6Co_2Ga and related compounds, and standardized with the program STRUCTURE TIDY.[17] The assignment of all sites was unequivocal except for the 2a site at the origin, which has been shown to accommodate a disordered distribution of atoms in other structure determinations. Various models were examined in which this site is occupied fully by Co, Bi, or a mixture of both atoms. Convergence and satisfactory residuals could only be obtained when this site was occupied fully by Co, resulting in the formula "$Ho_{24}Co_{10}Bi_2$" in the unit cell, or $Ho_{12}Co_5Bi$ with Z = 2. The final cycle of least-squares refinement included the scale factor, background, zero point, cell parameters, pseudo-Voigt peak profile parameters, atomic coordinates, and isotropic displacement parameters. The fit of the Rietveld refinement results to the powder pattern is shown in Figure 1. Final values of the positional and displacement parameters are given in Table 3. Interatomic distances are listed in Table 4.

Electrical Resistivity and Magnetic Susceptibility. All samples examined were phase-pure by powder X-ray diffraction. The electrical resistivity of polycrystalline samples of $(RE)_{12}Co_5Bi$ was measured between 2 and 300 K by standard four-probe techniques on a Quantum Design PPMS system equipped with an ac transport controller (model 7100). The current was 100 μA, and the frequency

(13) Kalychak, Ya. M.; Zaremba, V. I.; Stepien'-Damm, A.; Galadzhun, Ya. V.; Aksel'rud, L. G. *Crystallogr. Rep.* **1998**, *43*, 12−15.
(14) Gulay, L. D.; Kalychak, Ya. M.; Wołcyrz, M.; Łukaszewicz, K. *J. Alloys Compd.* **2000**, *311*, 238−240.
(15) Romaka, L.; Senkovska, O.; Fruchart, D.; Gignoux, D. *J. Magn. Magn. Mater.* **2002**, *242−245*, 854−857.
(16) Rodriguez-Carvajal, J. *FULLPROF: A Program for Rietveld Refinement and Pattern Matching Analysis*, version 3.5d; Laboratoire Léon Brillouin (CEA-CNRS): Saclay, France, 1998.
(17) Gelato, L. M.; Parthé, E. *J. Appl. Crystallogr.* **1987**, *20*, 139−143.

Table 2. Crystallographic Data for $Ho_{12}Co_5Bi$

empirical formula	$Ho_{12}Co_5Bi$
fw	2482.81
space group	*Immm* (No. 71)
a (Å)	9.37598(14)
b (Å)	9.37871(14)
c (Å)	9.85465(13)
V (Å^3)	866.57(2)
Z	2
ρ_{calcd} (g cm^{-3})	9.515
radiation	synchrotron, $\lambda = 0.699505$ Å
2θ range (deg)	5.0−67.9
step width (deg)	0.005
no. of data points	12578
no. of reflns	1057
no. of variables	27
residuals R_{Bragg}, Rp, wRp	0.048, 0.058, 0.088
goodness of fit, χ^2	4.97

Table 3. Positional and Isotropic Displacement Parameters for $Ho_{12}Co_5Bi$

atom	Wyckoff position	*x*	*y*	*z*	U_{iso} (Å^2)
Ho1	8n	0.1843(2)	0.2834(2)	0	0.0106(6)
Ho2	8m	0.1977(2)	0	0.2155(2)	0.0032(6)
Ho3	8l	0	0.3044(2)	0.3132(2)	0.0060(6)
Co1	4j	1/2	0	0.3874(6)	0.015(2)
Co2	4e	0.3767(6)	0	0	0.008(2)
Co3	2a	0	0	0	0.013(3)
Bi	2c	1/2	1/2	0	0.0055(10)

Table 4. Selected Interatomic Distances (Å) in $Ho_{12}Co_5Bi$

Ho1−Ho2	3.404(2) (×2)	Co1−Ho3	2.697(5) (×2)
Ho1−Ho1	3.455(3)	Co1−Ho1	2.888(3) (×4)
Ho1−Ho3	3.542(2) (×2)	Co1−Ho2	3.302(4) (×2)
Ho1−Ho3	3.582(2) (×2)	Co1−Co1	2.218(8)
Ho1−Ho2	3.635(2) (×2)	Co1−Co2	3.989(6) (×2)
Ho1−Co1	2.889(3) (×2)		
Ho1−Co3	3.170(2)	Co2−Ho2	2.707(4) (×2)
Ho1−Co2	3.212(4)	Co2−Ho3	2.845(3) (×4)
Ho1−Bi	3.590(2)	Co2−Ho1	3.212(4) (×2)
		Co2−Co2	2.312(8)
Ho2−Ho3	3.389(2) (×2)	Co2−Co3	3.532(6)
Ho2−Ho1	3.404(2) (×2)	Co2−Co1	3.989(6) (×2)
Ho2−Ho3	3.537(2) (×2)		
Ho2−Ho1	3.635(2) (×2)	Co3−Ho2	2.819(4) (×4)
Ho2−Ho2	3.707(3)	Co3−Ho1	3.170(2) (×4)
Ho2−Co2	2.707(4)	Co3−Ho3	4.204(4) (×2)
Ho2−Co3	2.819(2)	Co3−Co2	3.532(6) (×2)
Ho2−Co1	3.302(4)		
Ho2−Bi	3.360(2)	Bi−Ho2	3.360(2) (×4)
		Bi−Ho3	3.397(2) (×4)
Ho3−Ho2	3.389(2) (×2)	Bi−Ho1	3.590(2) (×4)
Ho3−Ho2	3.537(2) (×2)		
Ho3−Ho1	3.542(2) (×2)		
Ho3−Ho1	3.582(2) (×2)		
Ho3−Ho3	3.670(3)		
Ho3−Ho3	3.682(3)		
Ho3−Co1	2.697(5)		
Ho3−Co2	2.845(3) (×2)		
Ho3−Bi	3.397(2)		

was 16 Hz. Magnetic susceptibility measurements were made on ground samples (∼50 mg) between 2 and 300 K under an applied field of 0.5 T on a Quantum Design 9T-PPMS dc magnetometer/ac susceptometer. The susceptibility was corrected for contributions for the holder diamagnetism and the underlying sample diamagnetism.[18]

Band Structure. Tight-binding extended Hückel band structure calculations were performed with use of the EHMACC suite of programs.[19,20] Because the treatment of f orbitals is problematic in this method, the model considered was $Y_{12}Co_5Bi$, which has no f electrons. The lattice parameters were taken from $Y_{12}Co_5Bi$, and the positional parameters were assumed to be the same as in $Ho_{12}Co_5Bi$. The atomic parameters are listed in Table 5. Properties were extracted from the band structure using 125 *k*-points in the irreducible portion of the Brillouin zone.

Table 5. Extended Hückel Parameters

atom	orbital	H_{ii} (eV)	ζ_{i1}	c_1	ζ_{i2}	c_2
Y	5s	−6.82	1.39			
	5p	−4.30	1.39			
	4d	−6.56	4.33	0.5657	1.06	0.6575
Co	4s	−7.80	2.00			
	4p	−3.80	2.00			
	3d	−9.70	5.55	0.5550	1.90	0.6678
Bi	6s	−15.19	2.56			
	6p	−7.79	2.07			

Results and Discussion

Structure. The rare-earth intermetallics $(RE)_{12}Co_5Bi$ (RE = Y, Gd, Tb, Dy, Ho, Er, Tm) represent new members of the $(RE)_6M_{2+x}X_{1-x}$ family of compounds, previously known only for M = Co and Ni and X = Ga, In, Sn, and Pb.[1−9] Although the parent structure type Ho_6Co_2Ga is ordered,[1] subsequent structure determinations on the related compounds suggest that one of the atomic sites (2a), normally occupied by X atoms, is strongly susceptible to disorder with the M atoms, resulting in the nonstoichiometric formula $(RE)_6M_{2+x}X_{1-x}$, as occurs in $Ho_6Co_{2.135}In_{0.865}$ or $Tb_6Co_{2.35}Sn_{0.65}$, for example.[3,8] In the case of $Ho_{12}Co_5Bi$, the situation reaches an extreme when the 2a site now becomes fully occupied with Co atoms only, as shown in Table 3. The formula could be written as $Ho_6Co_{2.5}Bi_{0.5}$ to show the relationship with the other $(RE)_6M_{2+x}X_{1-x}$ compounds, but we prefer the formula $Ho_{12}Co_5Bi$ as it emphasizes the ordered nature of the structure. Further evidence for the correctness of this formula is provided by synthetic experiments, where the purest samples are obtained only at the ideal stoichiometry $Ho_{12}Co_5Bi$. When reactions are carried out with stoichiometries increasingly deviating from $Ho_{12}Co_5Bi$, impurity phases begin to be observed. In particular, a reaction carried out with the "Ho_6Co_2Bi" stoichiometry results in significant amounts of Ho_5Bi_3 and other phases.

The structure of $Ho_{12}Co_5Bi$ is shown in Figure 2 in two representations. Conventionally, Ho_6Co_2Ga-type structures have been regarded as being built up of a framework of RE atoms that define a set of space-filling polyhedra whose centers are occupied by the other component atoms.[1] Figure 2a shows that, in $Ho_{12}Co_5Bi$, there are compressed cuboctahedra and two types of distorted tetragonal antiprisms that are filled by Co atoms, icosahedra that are filled by Bi atoms, and empty octahedra. The elegant relationship of Ho_6Co_2Ga-type structures to other structures, such as WAl_{12} and

(18) Mulay, L. N., Boudreaux, E. A., Eds. *Theory and Applications of Molecular Diamagnetism*; Wiley-Interscience: New York, 1976.
(19) Whangbo, M.-H.; Hoffmann, R. *J. Am. Chem. Soc.* **1978**, *100*, 6093−6098.
(20) Hoffmann, R. *Solids and Surfaces: A Chemist's View of Bonding in Extended Structures*; VCH Publishers: New York, 1988.

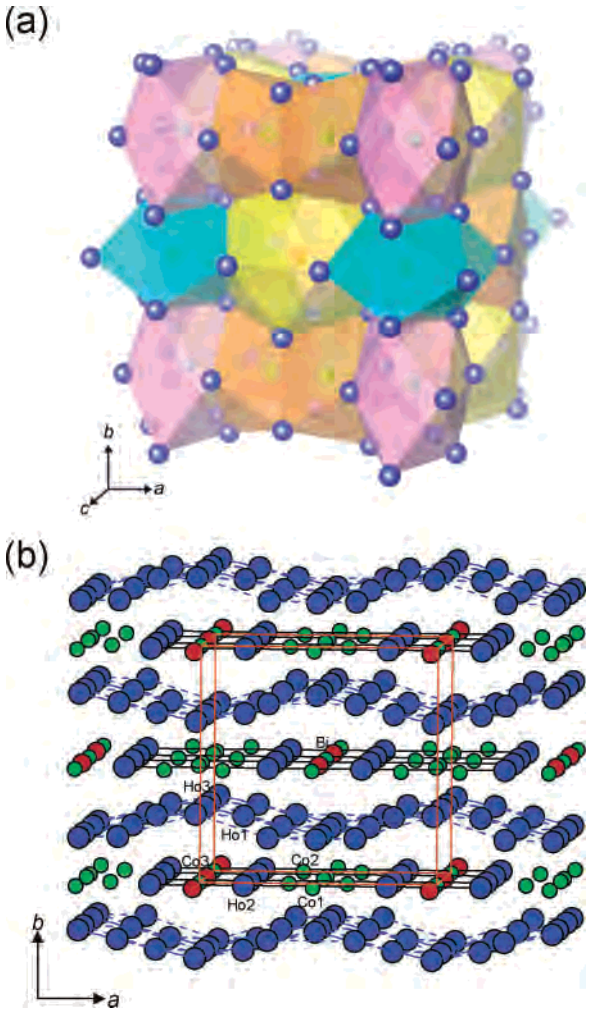

Figure 2. Structure of $Ho_{12}Co_5Bi$ in terms of (a) a polyhedral representation and (b) stacked nets of atoms. The large blue spheres are Ho atoms, the small green spheres are Co atoms, and the medium red spheres are Bi atoms. In (a), the Co1 and Co2 atoms are in cyan and orange tetragonal antiprisms, respectively, the Co3 atoms are in magenta cuboctahedra, and the Bi atoms are in yellow icosahedra.

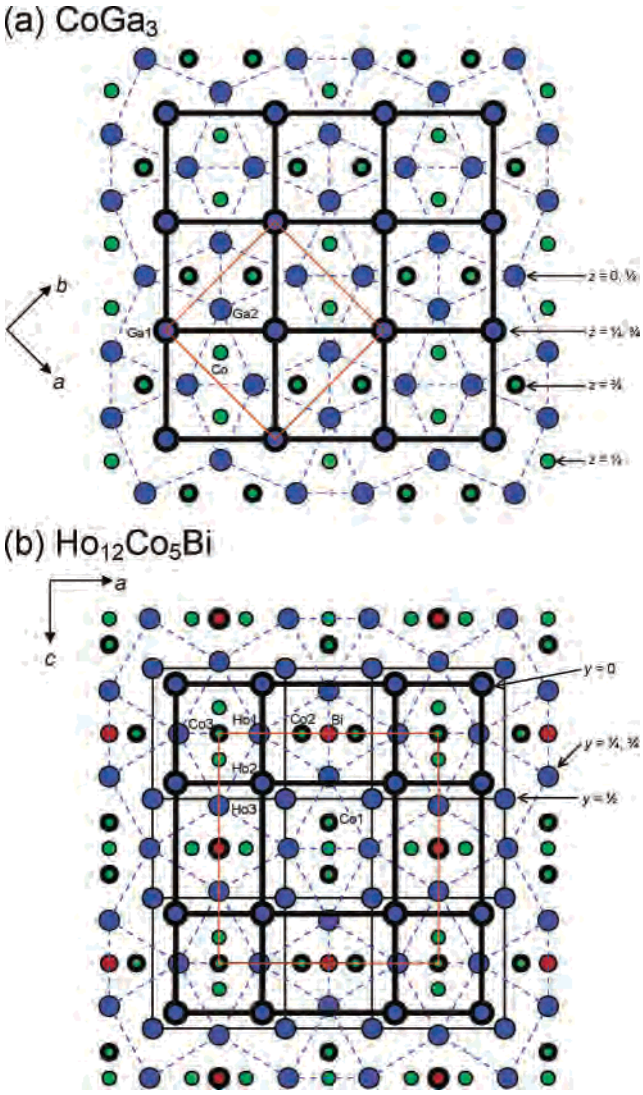

Figure 3. Comparison of the structures of (a) $CoGa_3$ and (b) $Ho_{12}Co_5Bi$ in terms of interleaved 3^2434 (dashed lines) and 4^4 (solid lines) nets, projected down the stacking axis and with the unit cell outlined in orange. The heights of atoms along the projection axis are indicated.

the now popular skutterudite structures, based on the occupation of these polyhedra, has been discussed previously.[1]

We augment this description by drawing attention to the stacking of nets, arguably the most successful means of systematically classifying the structures of intermetallic solids, and point out additional relationships. Figure 2b shows that, in $Ho_{12}Co_5Bi$, the Ho atoms are arranged in 3^2434 and 4^4 nets that are alternately stacked along the *b* direction, with Co and Bi atoms occupying interstitial sites. Although perhaps less familiar than 3^6 (close packed) nets, these nets form the basis for many intermetallic structures.[21] As shown in Figure 3, the structure of $Ho_{12}Co_5Bi$ is related to that of $CoGa_3$.[22] In $CoGa_3$, 3^2434 nets of Ga atoms are stacked directly above each other and are interleaved by 4^4 nets of Ga atoms, with Co atoms situated above or below the triangles of the 3^2434 nets. In $Ho_{12}Co_5Bi$, 3^2434 nets of Ho atoms are stacked directly above each other and are interleaved by irregular 4^4 nets of Ho atoms, with Co atoms situated above or below the triangles and Bi atoms situated above or below the diamonds of the 3^2434 nets.

On the basis of filling interstitial sites between these two types of nets, the compositions and structures of several ternary rare-earth-rich intermetallics can be more easily understood, as summarized in Table 6. The evolution from Ho_6Co_2Ga to $Ho_{12}Co_5Bi$ proceeds with the p-block atoms (X) in the cuboctahedral sites being gradually replaced by transition-metal atoms (M). In $Sm_{12}Ni_6In$, the cuboctahedral sites are empty but the adjacent tetragonal antiprismatic sites are occupied by additional transition-metal atoms.[13] As shown in Figure 4, the structure of Ho_5Ni_2Sb (and other RE_5M_2X compounds with the Mo_5B_2Si-type structure) has strictly planar 3^2434 nets stacked in an ABBA sequence,[23−25]

(21) Pearson, W. B. *The Crystal Chemistry and Physics of Metals and Alloys*; Wiley-Interscience: New York, 1972.
(22) Schubert, K.; Lukas, H. L.; Meissner, H.-G.; Bhan, S. *Z. Metallkd.* **1959**, *50*, 534−540.
(23) Mozharivskyj, Yu.; Franzen, H. F. *J. Solid State Chem.* **2000**, *152*, 478−485.
(24) Mozharivskyj, Yu. A.; Kuz'ma, Yu. B.; Sichevich, O. M. *Inorg. Mater. (Engl. Transl.)* **1998**, *34*, 707−710.

Table 6. Relationship among Ternary Rare-Earth-Rich Intermetallic Compounds

	$8(Ga_3Co) = Ga_{24}Co_8$	$4(Ho_6Co_2Ga) = Ho_{24}Co_8Ga_4$	$4((RE)_6M_{2+x}X_{1-x}) = (RE)_{24}M_{4(2+x)}X_{4(1-x)}$	$2(Ho_{12}Co_5Bi) = Ho_{24}Co_{10}Bi_2$	$2(Sm_{12}Ni_6In) = Sm_{24}Ni_{12}In_2$	$4(Ho_5Ni_2Sb) = Ho_{20}Ni_8Sb_4$[a]
3^2434 nets	16 Ga	16 Ho	16 RE	16 Ho	16 Sm	16 Ho
4^4 nets	8 Ga	8 Ho	8 RE	8 Ho	8 Sm	4 Ho + 4 Sb
tetragonal antiprismatic sites	8 Co	8 Co	8 M	8 Co	12 Ni	8 Ni
cuboctahedral sites		2 Ga	$(4x)$ M + $(2 - 4x)$ X	2 Co		
icosahedral sites		2 Ga	2 X	2 Bi	2 In	
reference	22	1	3−5	this work	13	22

[a] Here, the 3^2434 nets are arranged in a stacking sequence of ABBA, unlike the other compounds, where they are stacked AAAA.

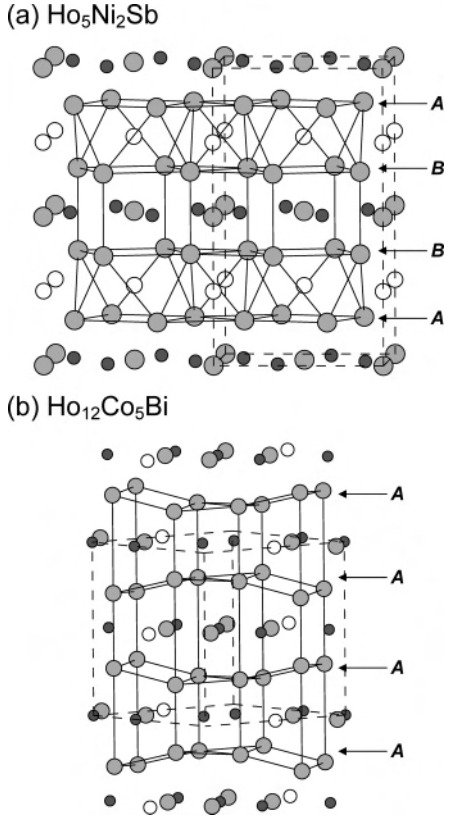

Figure 4. Comparison of the structures of (a) Ho_5Ni_2Sb and (b) $Ho_{12}Co_5Bi$ in terms of the stacking sequence of 3^2434 nets of Ho atoms. The large lightly shaded circles are Ho atoms, the small solid circles are Ni or Co atoms, and the medium open circles are Sb or Bi atoms.

in contrast to that of $Ho_{12}Co_5Bi$ and other Ho_6Co_2Ga-related structures where the 3^2434 nets are corrugated and stacked directly on top of each other, in an AAAA sequence.

Inspection of the interatomic distances (Table 4) immediately reveals why the cuboctahedral site (in the polyhedral description), which normally houses the main-group component atom X in $(RE)_6M_{2+x}X_{1-x}$ compounds, is occupied by Co3 and not Bi atoms in $Ho_{12}Co_5Bi$: the 2.819(4) Å (×4) distances are simply too short to accommodate the large Bi atoms. The interatomic distances generally agree well with the sum of the metallic radii ($R(L12)$: Ho, 1.76 Å; Co, 1.25 Å; Bi, 1.78 Å).[26] However, the Co1−Co1 distance of 2.218(8) Å, across the shared face of two tetragonal antiprisms, is very short. This appears to be a recurring feature of all Co representatives of $(RE)_6$-$M_{2+x}X_{1-x}$ compounds, where crystal structures have been determined.

Table 7. Summary of Magnetic Data for $(RE)_{12}Co_5Bi$ (RE = Gd−Tm)

compound	μ_{eff} (μ_B/(RE)$^{3+}$)	μ_{RS} (μ_B/(RE)$^{3+}$)	θ_P (K)	T_N (K)
$Gd_{12}Co_5Bi$	7.72	7.94	111.9	118.2[a]
$Tb_{12}Co_5Bi$	10.34	9.72	43.2	74.7
$Dy_{12}Co_5Bi$	11.71	10.65	14.4	39.8
$Ho_{12}Co_5Bi$	10.95	10.61	5.6	15.9
$Er_{12}Co_5Bi$	9.36	9.58	0.4	6.9
$Tm_{12}Co_5Bi$	7.68	7.56	−4.0	2.7

[a] Transition temperature for proposed ferrimagnetic ordering.

Properties. The high content of atoms carrying a magnetic moment in $(RE)_{12}Co_5Bi$ compounds suggests that interesting transport and magnetic properties may be anticipated. Electrical resistivity and magnetic susceptibility measurements were carried out on all members of the $(RE)_{12}Co_5Bi$ series. All $(RE)_{12}Co_5Bi$ compounds display metallic behavior, but transitions are observed in the resistivity and susceptibility curves as a function of temperature. Except for $Y_{12}Co_5Bi$, all other $(RE)_{12}Co_5Bi$ compounds obey the Curie−Weiss law at high temperature and undergo a magnetic ordering transition at lower temperature. These magnetic data are summarized in Table 7.

$Y_{12}Co_5Bi$. The electrical resistivity decreases relatively smoothly with decreasing temperature and levels off to a residual value of 320 $\mu\Omega\cdot$cm at low temperature (Figure 5a). The dc magnetic susceptibility exhibits a non-Curie−Weiss temperature dependence and reaches a cusplike maximum at 2.6 K (Figure 5b). At all temperatures, the field-cooled and zero-field-cooled susceptibility curves diverge, implying a significant irreversibility in the alignment of moments. At a temperature below this maximum, the isothermal magnetization curve shows ferromagnetic-like behavior, with the magnetization increasing rapidly and not reaching saturation at fields up to 9 T (Figure 5c). Measurements of the ac magnetic susceptibility at different frequencies reveal a complex profile for this transition, which shifts to lower temperatures with higher frequency (Figure 5d). A possible model is a spin-glass system with a freezing temperature, T_f, of 2.6 K, below which magnetic moments are frozen into a random arrangement because of variable coupling between atoms arising from disorder or frustration. However, some of the observations are not characteristic of conventional spin glasses, which normally display Curie−Weiss behavior above T_f and which show divergence of the field-cooled and zero-field-cooled susceptibility only below T_f. Given that Y^{3+} is nonmagnetic and the Co atoms probably have negligible magnetic moments (because the good agreement between

(25) Mozharivskyj, Yu.; Franzen, H. F. *J. Alloys Compd.* **2001**, *327*, 78−81.
(26) Pauling, L. *The Nature of the Chemical Bond*, 3rd ed.; Cornell University Press: Ithaca, NY, 1960.

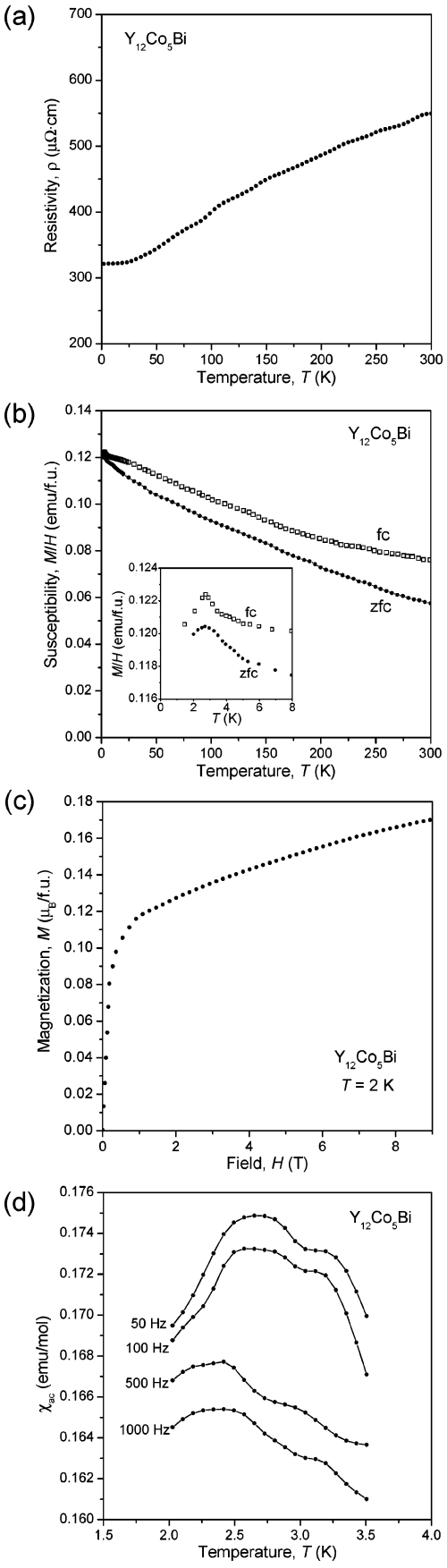

Figure 5. $Y_{12}Co_5Bi$: (a) electrical resistivity, (b) field-cooled (fc) and zero-field-cooled (zfc) dc magnetic susceptibility (inset: low-temperature behavior), (c) isothermal magnetization at 2 K, and (d) ac magnetic susceptibility (real component) at various frequencies.

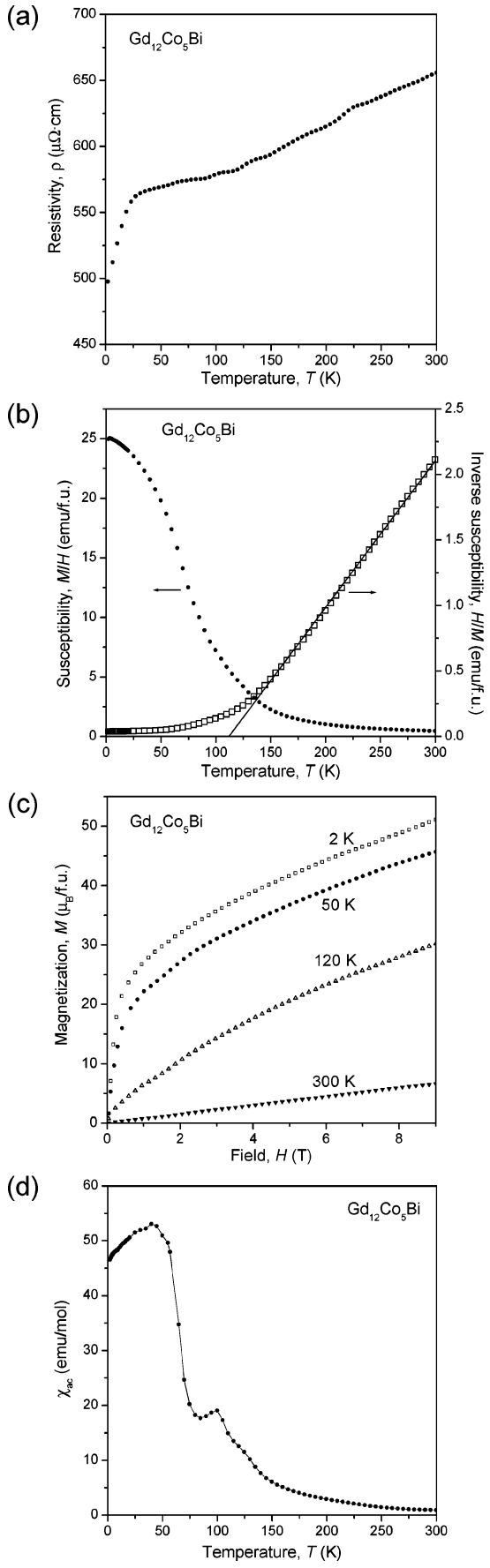

Figure 6. $Gd_{12}Co_5Bi$: (a) electrical resistivity, (b) dc magnetic susceptibility and its inverse, (c) isothermal magnetization at various temperatures, and (d) ac magnetic susceptibility (real component) at 1000 Hz.

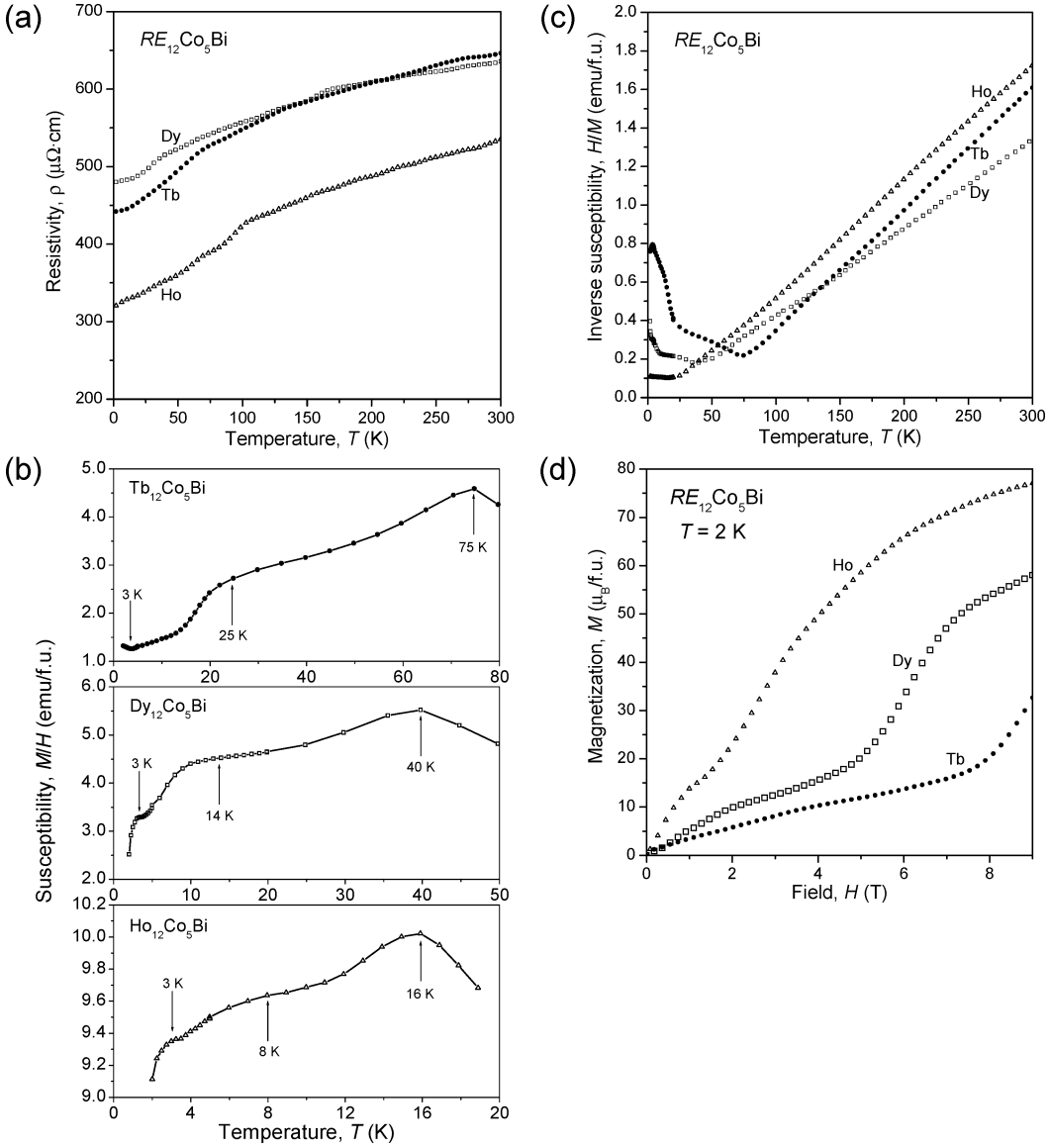

Figure 7. $Tb_{12}Co_5Bi$, $Dy_{12}Co_5Bi$, and $Ho_{12}Co_5Bi$: (a) electrical resistivity, (b) dc magnetic susceptibility at low temperatures, (c) inverse dc magnetic susceptibility, and (d) isothermal magnetization at 2 K.

effective magnetic moments for other members of the $(RE)_{12}Co_5Bi$ series to the free-ion values for $(RE)^{3+}$ (Table 7) implies that there is little contribution from Co), it is unclear how to account for the spin-glass-like behavior. The condition of a dilute magnetic system could be satisfied if disorder is introduced by allowing small local moments to be present on some of the Co sites that may be susceptible to partial occupancy (such as Co1 or Co2, where anomalously short Co−Co contacts are formed).

$Gd_{12}Co_5Bi$. The dramatic decrease in the electrical resistivity below 30 K (Figure 6a) implies a loss of some conduction electron scattering mechanism, but the dc magnetic susceptibility plot shows no corresponding transition at the same temperature (Figure 6b). Instead, the dc magnetic susceptibility is well described by the Curie−Weiss law with $\mu_{eff} = 7.72\ \mu_B/Gd^{3+}$ (close to the free-ion moment of 7.94 μ_B for Gd^{3+}) and $\theta_P = 111.9$ K in the high-temperature regime. Below 120 K, the susceptibility rises rapidly and exceeds what would be expected from Curie−Weiss behavior. This suggests that an onset of perhaps ferrimagnetic ordering is occurring at 120 K, supported by isothermal magnetization curves (Figure 6c) which reveal an increasing curvature below this temperature. The ac magnetic susceptibility reveals both of these transitions (Figure 6d), at somewhat different temperatures (40 and 100 K, respectively), although the effect of small amounts of impurities has not been ruled out. The electrical and magnetic behavior of $Gd_{12}Co_5Bi$ resembles that of Gd_6Co_2Ga,[2] which has been proposed to undergo ferrimagnetic ordering, but at a considerably higher temperature, ~180 K.

$Tb_{12}Co_5Bi$, $Dy_{12}Co_5Bi$, and $Ho_{12}Co_5Bi$. The electrical resistivities of these three compounds show complicated temperature dependence (Figure 7a). For $Tb_{12}Co_5Bi$ and $Dy_{12}Co_5Bi$, there are transitions in the electrical resistivity curves at 75 and 40 K, respectively, that correspond to maxima at T_N in the dc magnetic susceptibility curves (Figure 7b). The sharper decrease in resistivity below these temperatures results from a loss of spin-disorder scattering as long-range

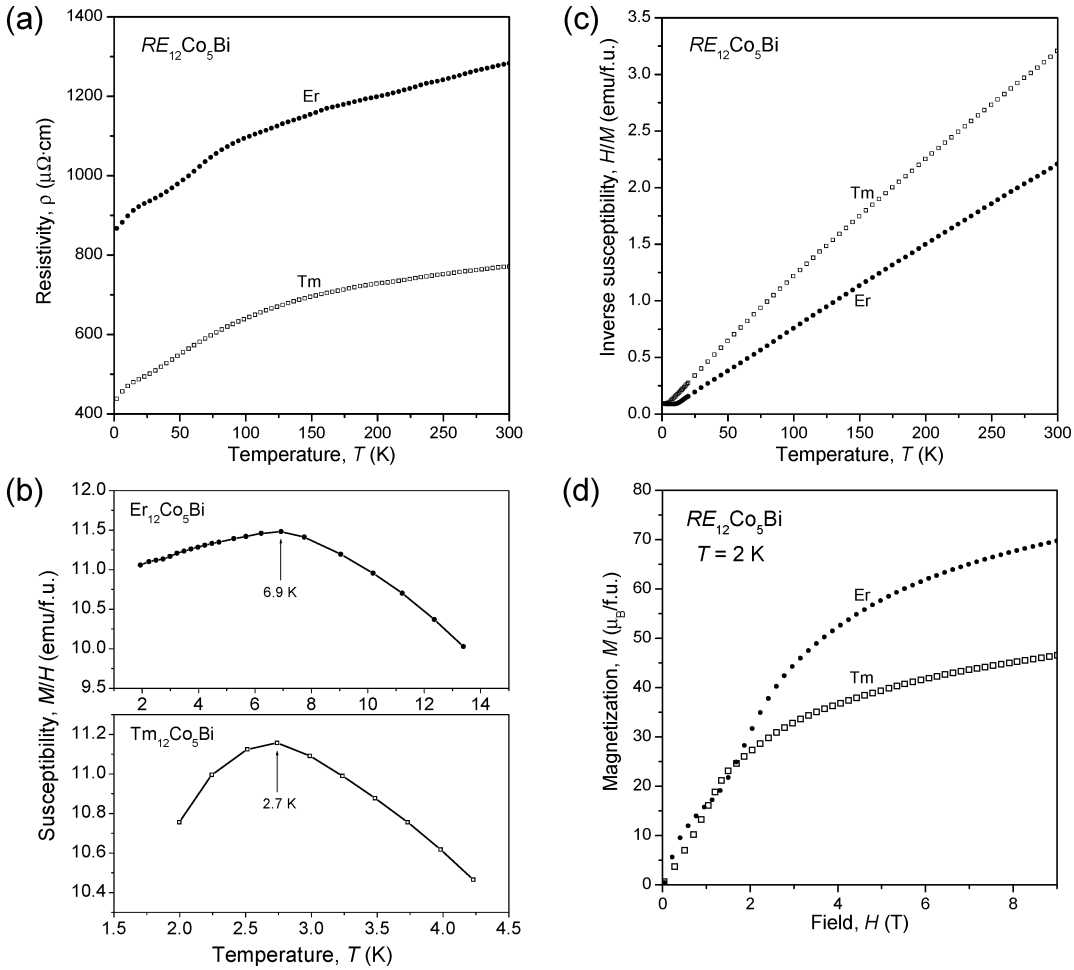

Figure 8. $Er_{12}Co_5Bi$ and $Tm_{12}Co_5Bi$: (a) electrical resistivity, (b) dc magnetic susceptibility at low temperatures, (c) inverse dc magnetic susceptibility, and (d) isothermal magnetization at 2 K.

magnetic ordering sets in, although it is puzzling why the 16 K transition observed in the dc magnetic susceptibility for $Ho_{12}Co_5Bi$ is not manifested by a similar effect on the resistivity curve. There are two additional transitions at even lower temperatures below T_N in the dc magnetic susceptibility, at 25 and 3 K for $Tb_{12}Co_5Bi$, 14 and 3 K for $Dy_{12}Co_5Bi$, and 8 and 3 K for $Ho_{12}Co_5Bi$. These transitions resemble those found in Er_6Ni_2Sn, where the onset of two antiferromagnetically ordered phases is proposed.[7] Above the transition temperatures, the linear dependence of the inverse dc magnetic susceptibility (Figure 7c) can be fitted well to the Curie−Weiss law, giving effective magnetic moments that can be compared with the free-ion values for the ground-state configurations of $(RE)^{3+}$ (Table 7). If the contribution of Co atoms to the effective magnetic moment is assumed to be negligible, then the effective magnetic moments for $Tb_{12}Co_5Bi$ (10.34 μ_B/Tb^{3+}) and $Dy_{12}Co_5Bi$ (11.71 μ_B/Dy^{3+}) are about 1 μ_B higher than expected for the free-ion values for Tb^{3+} (9.72 μ_B) and Dy^{3+} (10.65 μ_B). The enhancement of the effective magnetic moments may arise from polarization of RE 5d states. A similar situation is observed in Er_6Ni_2Sn.[7] The magnetization curves at 2 K reveal metamagnetic behavior (Figure 7d), with the antiferromagnetic structure collapsing when the applied magnetic field exceeds $H_c = 8$, 5, and 2 T for $Tb_{12}Co_5Bi$, $Dy_{12}Co_5Bi$, and $Ho_{12}Co_5Bi$, respectively, followed by an approach to saturation.

$Er_{12}Co_5Bi$ and $Tm_{12}Co_5Bi$. The electrical resistivity (Figure 8a) and dc magnetic susceptibility behavior (Figure 8b) are slightly less complicated than those of the previous members. There is now only one maximum in the dc magnetic susceptibility corresponding to T_N, and there appear to be no other magnetic phases at lower temperatures. A fit of the inverse magnetic susceptibility to the Curie−Weiss law (Figure 8c) leads to effective magnetic moments for $Er_{12}Co_5Bi$ (9.36 μ_B/Er^{3+}) and $Tm_{12}Co_5Bi$ (7.68 μ_B/Tm^{3+}) that are in good agreement with the free-ion values for Er^{3+} (9.58 μ_B) and Tm^{3+} (7.56 μ_B). As before, there is a metamagnetic transition but at lower critical fields; $H_C = 1.5$ and 1 T for $Er_{12}Co_5Bi$ and $Tm_{12}Co_5Bi$, respectively (Figure 8d).

Although there is a wide range of magnetic behavior in the $(RE)_{12}Co_5Bi$ series, the essential type of interaction is antiferromagnetic coupling between the RE moments. As Figure 9 shows, the magnetic ordering temperature is found to be closely proportional to the de Gennes factor, $(g - 1)^2(J(J + 1))$, which scales as the strength of the magnetic coupling between local RE moments interacting through the intermediary of conduction electrons (RKKY interactions). The implication is that the electronic structures are similar

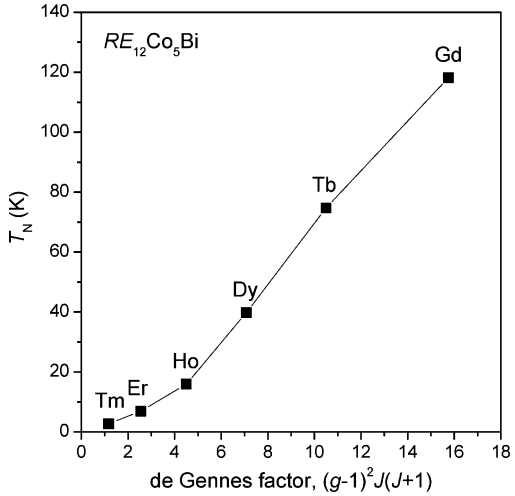

Figure 9. Magnetic ordering temperature for $(RE)_{12}Co_5Bi$ compounds versus the de Gennes factor.

for all compounds, and this is supported by the gross resemblance of the magnitudes and dependence of the electrical resistivities. Similar correlations in the magnetic ordering temperatures have been observed for compounds related to $(RE)_{12}Co_5Bi$ such as $(RE)_6Ni_2Sn$ and $(RE)_{12}Ni_6Sn$.[2,15]

Bonding. To a first approximation, the most important bonding component in $(RE)_{12}Co_5Bi$ compounds may be expected to involve interactions between the more electropositive RE and the more electronegative Co atoms. These polar intermetallic bonds can be rationalized in terms of a Lewis acid−base stabilization, first proposed for binary transition-metal alloys between early and late transition metals.[27] After formation of RE−Co bonds, any remaining electrons are then used to form RE−RE bonds. The minor constituent Bi acts as an interstitial atom that plays only a minimal role in stabilizing the structure.

These expectations are verified by band structure calculations on $Y_{12}Co_5Bi$, where f orbitals can be neglected. Figure 10 shows the density of states (DOS) and its projections for $Y_{12}Co_5Bi$. There is significant mixing of Y and Co states in the region from −11.5 eV up to the Fermi level at −7.9 eV. Electron transfer occurs from Y to Co atoms, as confirmed by the calculated atomic charges of +0.27 for Y and −1.11 for Co. Above the Fermi level, the density of states largely comprises contributions from Y states. The Bi contribution to the DOS is minimal and restricted to a small energy region roughly between −9 and −11 eV, implying that bonding to Bi atoms is highly localized. The crystal orbital overlap population (COOP) curves (Figure 11) reveal that Y−Co and Y−Bi bonding is optimized, with all essentially bonding levels just occupied up to the Fermi level, but there are still additional Y−Y bonding levels above the Fermi level. The Mulliken overlap populations are 0.21 for Y−Y (3.4−3.8 Å), 0.17 for Y−Co (2.7−3.3 Å), and 0.26 for Y−Bi (3.4−3.6 Å). These values and the general features of the band structure are similar to those found in Y_5Ni_2Sb (which was used to model Ho_5Ni_2Sb),[23] even though it adopts a structure with a different stacking sequence of 3^2434 nets. Interestingly, the short Co1−Co1 and Co2−Co2 distances (2.2−2.3 Å) in $Y_{12}Co_5Bi$, which were noted earlier as a recurring feature of all Co-containing $(RE)_6M_{2+x}X_{1-x}$ compounds, are found to correspond to Mulliken overlap populations of 0.14−0.19, less than half of what would be expected for a bona fide Co−Co single bond. As well, the COOP curve for these Co−Co contacts shows that the occupation of antibonding levels cancels out the effect of the bonding levels (Figure 10d). This confirms that matrix effects, and not favorable orbital overlap, are likely responsible for the anomalous shortness of these Co−Co contacts.

Although the results of the band structure calculation are helpful in understanding many features of bonding in the $(RE)_{12}Co_5Bi$ compounds, it is difficult to apply these results to explain their properties, other than the trivial prediction that they should be metallic. A more rigorous calculation, involving spin polarization and including the f orbitals, is necessary to gain insight into the magnetic properties of these compounds.

Conclusion

The new series of rare-earth intermetallic compounds $(RE)_{12}Co_5Bi$ presents a complex structure that gives rise to a rich variety of electrical and magnetic properties. The electronic structure is dominated by RE and Co states, and

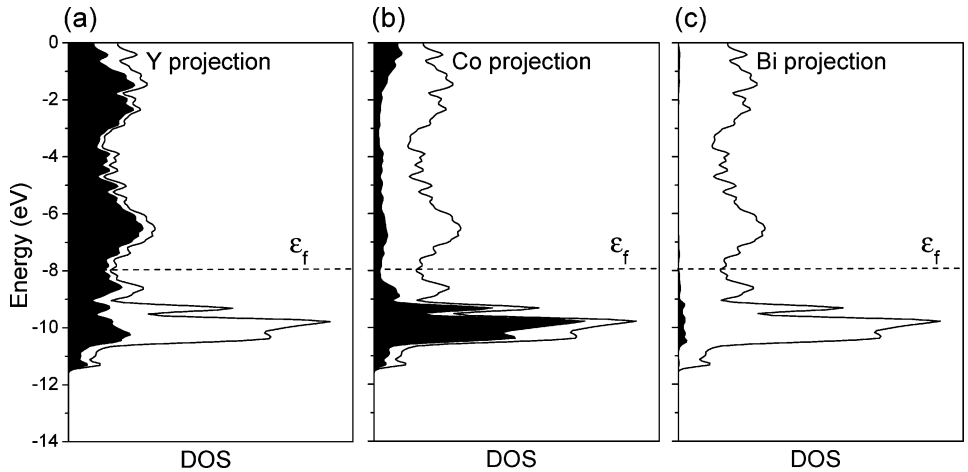

Figure 10. Contributions of (a) Y, (b) Co, and (c) Bi (shaded regions) to the total density of states (DOS) (line) for $Y_{12}Co_5Bi$. The horizontal line marks the Fermi level ($\epsilon_f = -7.9$ eV).

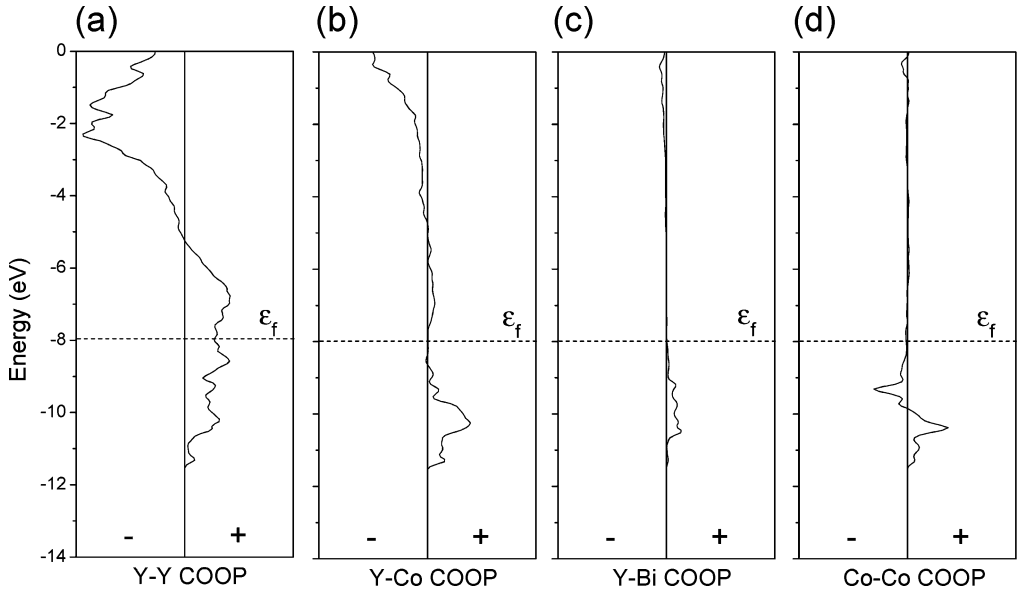

Figure 11. Crystal orbital overlap population (COOP) curves for (a) Y−Y, (b) Y−Co, (c) Y−Bi, and (d) Co−Co interactions (<4.0 Å) in $Y_{12}Co_5Bi$.

magnetic ordering originates from coupling of RE moments mediated through conduction electrons. Further investigation, such as heat capacity measurements and neutron diffraction experiments, is desirable to characterize these properties more fully, given the multitude of transitions observed in the electrical and magnetic behavior.

Acknowledgment. The Natural Sciences and Engineering Research Council of Canada and the University of Alberta supported this work. Research was carried out in part at the National Synchrotron Light Source (NSLS) at Brookhaven National Laboratory, which is supported by the U.S. Department of Energy, Division of Materials Sciences and Division of Chemical Sciences. The SUNY X3 beamline at the NSLS was previously supported by the Division of Basic Energy Sciences of the U.S. Department of Energy under Grant No. DF-FG02-86ER45231. We are grateful to Dr. Peter W. Stephens (SUNY Stony Brook) and Dr. Ronald Cavell (University of Alberta) for technical assistance and helpful discussions, and we thank the ASI (Alberta Synchrotron Institute) and CLS (Canadian Light Source) for facilitating access to the NSLS.

Supporting Information Available: X-ray crystallographic data in CIF format. This material is available free of charge via the Internet at http://pubs.acs.org.

(27) Brewer, L.; Wengert, P. R. *Metall. Trans.* **1973**, *4*, 83−104.

IC048195P